Asteroid 2008 TC_3 – Almahata Sitta: A spectacular breccia containing many different ureilitic and chondritic lithologies.

Addi Bischoff[1], Marian Horstmann[1], Andreas Pack[2], Matthias Laubenstein[3], and Siegfried Haberer[4]

[1]Institut für Planetologie, Wilhelm-Klemm-Str. 10, D-48149 Münster, Germany (e-mail: bischoa@uni-muenster.de)

[2]Universität Göttingen, Geowissenschaftliches Zentrum, Goldschmidtstrasse 1, D-37077 Göttingen, Germany

[3]Laboratori Nazionali del Gran Sasso - I.N.F.N., S.S.17/bis, km 18+910, I-67010 Assergi (AQ), Italy

[4]Haberer-Meteorites, Ruhbankweg 15, D-79111 Freiburg, Germany

Meteoritics & Planetary Science

(submitted Feb. 24, 2010)

Abstract

Asteroid 2008 TC_3 impacted the Earth in northern Sudan October 7, 2008. The meteorite named Almahata Sitta was classified as a polymict ureilite. In this study 40 small pieces from different fragments collected in the Almahata Sitta strewn field were investigated and a large number of different lithologies was found. Some of these fragments are ureilitic in origin, whereas others are clearly chondritic. Since all are relatively fresh and because short-lived cosmogenic radioisotopes were detected within two of the chondritic fragments, we are convinced that most, if not all belong to the Almahata Sitta meteorite fall. The fragments can roughly be subdivided into achondritic (ureilitic; 23 samples) and chondritic lithologies (17 samples). Among the ureilitic rocks are at least 10 different lithologies. A similar number of different chondritic lithologies also exist. Most chondritic fragments belong to at least seven different E chondrite rock types (EH3, EL3/4, EL6 breccia, EL6, EL5/6, EH5, shock-darkened EH4/5 chondrites), but also two H-group ordinary chondrite lithologies were detected as well as one sample of a so far unique type of chondrite. Oxygen isotope compositions of several fragments provide further fundamental information on the lithological heterogeneity of the Almahata Sitta meteorite. Based on the findings presented in this paper the reflectance spectrum of asteroid 2008 TC_3 has to be evaluated in a new light.

Introduction:

Asteroid 2008 TC_3 was the first asteroid detected in space and impacting the Earth in the Nubian Desert of northern Sudan October 7, 2008. Hundreds of mostly small fragments were recovered. The meteorite called Almahata Sitta was classified as a polymict ureilite (Jenniskens et al., 2009) based on the study of only one meteorite fragment from the strewn field. The analysis by these authors shows that this meteorite is "an achondrite, a polymict ureilite, anomalous in its class: ultra-fine-grained and porous, with large carbonaceous grains". We have studied 40 small pieces from different fragments collected in the Almahata Sitta strewn field and found a large number of different lithologies. Some of these fragments are ureilitic in origin, whereas others are clearly chondritic. Since all are relatively fresh, we are convinced that most, if not all belong to the Almahata Sitta meteorite fall.

Here, we will present mineralogical and oxygen isotope data on several Almahata Sitta meteorite fragments and the results of a study of short-lived cosmogenic radioisotopes on two chondritic fragments. Some preliminary data has been published by Bischoff et al. (2010) and Horstmann and Bischoff (2010).

Sample and Analytical Techniques:

All 40 studied Almahata Sitta fragments were found as fresh complete meteorite fragments of 2.6 - 50 g in the Almahata Sitta strewn field. A small piece of all these fragments was selected for thin section preparation. Two sliced or partly sliced fragments of 5.1 g (MS-CH) and 8.65 g (MS-D) were used to measure the short-lived nuclides at the Laboratori Nazionali del Gran Sasso (LNGS) (Italy). Small grains from several different fragments (with less than 5 mg) were prepared for oxygen isotope measurements at the Universität Göttingen (Germany).

The mineralogy and texture of the fragments were studied by light and electron optical microscopy. A JEOL 6610-LV electron microscope was used to resolve the fine-grained textures and to analyze the mineral constituents using the EDS attached (INCA; Oxford Instruments). As natural standards we used olivine (Mg, Fe, Si), jadeite (Na), plagioclase (Al), sanidine (K), diopside (Ca), rutile (Ti), chromite (Cr), rhodonite (Mn), and pentlandite (Ni).

The oxygen isotope composition was measured by laser fluorination gas mass spectrometry. Sample material (typically ~1 mg) is reacted with purified F_2 gas with aid of a 50 W infrared laser. Excess F_2 is reacted to Cl_2 in a NaCl trap and Cl_2 is trapped in a cold trap (-196°C). Sample O_2 is analyzed in continuous flow mode with a ThermoElectron MAT 253 gas mass spectrometer. Accuracy and precision in $\delta^{18}O$ and $\Delta^{17}O$ are typically ±0.2 and ±0.06 ‰. The terrestrial fractionation line is defined by 290 analyses of rocks and minerals to $\beta = 0.5250 \pm 0.0007$ (1σ).

The short lived cosmogenic radioisotopes of two chondritic fragments from the Almahata Sitta strewn field were measured by means of γ-ray spectroscopy. The measurements were performed using high purity Germanium (HPGe) detectors, in ultra low background configuration (25 cm of lead and an inner liner of 5 cm copper, inside an underground laboratory with 1400 m rock overburden). The counting efficiency was determined with a thoroughly tested Monte-Carlo code. The samples have been measured from 13.10.2009 –

18.10.2009 in the case of the sample MS-CH, and from 09.11.2009 – 06.12.2009 in the case of the sample MS-D.

Results:

In this paper we will present mineralogical and oxygen isotope data, as well as the characteristics of a cosmogenic radioisotope study on various meteorite fragments of the Almahata Sitta strewn field. The fragments can roughly be subdivided into achondritic (ureilitic; 23 samples) and chondritic lithologies (17 samples). Main mineralogical characteristics are given in Tables 1 and 2. Details on some fragments have been previously presented by Bischoff et al. (2010) and Horstmann and Bischoff (2010). Please note that the statistic of different lithological objects presented in Tables 1 and 2 may not be representative for the real distribution of collected fragments.

Mineralogy - ureilitic lithologies

Among the samples are **9 ultra-fine-grained ureilites** and **11 or 12 coarse-grained ureilites.** One of the coarse-grained specimens may not be a real ureilitic lithology as described below. Two fragments are dominated by **metal-sulfide intergrowth** having ureilitic lithologies attached or enclosed:

The fragments of the **fine-grained variety** are mineralogically similar to those described by Jenniskens et al. (2009), Zolensky et al. (2009), and Herrin et al. (2009). Typical individual olivine grains within these fragments are always below 30 µm, in many cases below 20 µm (Figs. 1a-c and 1f; Tab. 1). The fine-grained texture of fragment MS-168 is shown in Fig. 1f. Low-Ca pyroxene often occurs intergrown with olivine, Ca-pyroxene, and troilite. Ca-pyroxene is mostly an interstitial phase, and FeS and kamacite occur as grains of variable grain size. Although the bulk fragments are similar in texture among each other, they vary in mineral composition from fragment to fragment (Tab. 1). Some have a mean olivine composition of ~Fa_{12-14} (e.g., MS-61, MS-152), whereas others can have mean olivine compositions between ~Fa_3 (e.g., MS-154) and ~Fa_{18} (e.g., MS-161; Fig. 1a). One fragment (MS-152), mainly having olivine of Fa_{12-14}, includes a highly reduced clast with ~Fa_1 olivines (Fig. 1b). In another case a fine-grained ureilitic fragment contains a fragment with a significantly larger grain size compared to the surroundings (MS-124; Fig. 1c). The cores of the olivine within the coarser-grained fragment (~Fa_{18-20}) have a similar composition to those of the fine-grained lithology (~Fa_{19-21}).

Fragment MS-165 is a niningerite-bearing, fine-grained ureilite (Fig. 1d). Within this fragment, which is dominated by fine-grained ureilitic lithologies, an area was identified, which contains abundant niningerite and metals that have compositions (Ni: ~3.5 wt%, Si: ~4.4 wt%; Co: ~0.3 wt%) similar to those in EH-chondrites. As additional phases low-Ca pyroxene (up to En_{99}), Cr-bearing troilite, and a SiO_2-phase were found. Grains of SiO_2 in ureilites were previously reported to occur within the reduced olivine rims (e.g., Weber et al., 2003). A similar specimen is fragment MS-20 containing metal-rich areas having opaques similar to those found in enstatite chondrites: Niningerite, troilite, and metals with about 3.5 wt% Si and ~5.5 wt% Ni (Fig. 1e).

Based on texture and mineral compositions the **coarse-grained ureilites** belong to at least six different lithologies of the parent body (Fig. 2). They all have typical grain sizes in excess of 100-300 µm, some are very coarse-grained with olivine grains up to several mm in size (Table 1). The Table also contains the compositions of olivine and pyroxene of the samples.

Some fragments represent typical ureilites (e.g., MS-160 (Fig. 2a), MS-162, MS-157, MS-167 (Fig. 2b), MS-170). The mm-sized olivines within these ureilites have cores of ~Fa_{18-23} and reduced rims (down to ~Fa_1; Table 1). Four fragments have abundant pyroxene (MS-16, MS-169 (Fig. 3a), MS-173, MS-175 (Fig. 2c,d)) and the olivines in these fragments have cores with lower fayalite contents (~Fa_6 - ~Fa_{11-14}) than those within the typical coarse-grained, pyroxene-poor variety (Table 1). In fragment MS-16, pyroxene is by far the dominating phase (>80 vol%; Fig. 3b). Based on the mineralogy it is not certain, weather this rock represents an ureilitic lithology or not. The low-Ca pyroxenes are quite uniform in composition (~Fs_{5-6}), whereas the olivines have cores with approximately Fa_{5-6}, but show some zoning (Table 1). The metals within the samples have about 4-5 wt% Ni. However, based on the oxygen isotope composition it falls within the ureilite field (see below).

Fragment MS-156 represents a unique type of ureilitic lithology. The huge olivine grains (Fig. 3c) have a remarkable internal texture with zoned olivines and a fine-grained network of FeS and metals with variable Ni-concentrations (Fig. 3d). The cores of the olivines are ~Fa_{19}, whereas the olivine close to the sulfide/metal assemblage is $Fa_{<10}$ (Fig. 3d). The Almahata Sitta fragments MS-153 (Fig. 3e) and MS-171 (Fig. 3f) are distinctly smaller-grained (typical grain size: 100-300 µm; Table 1) than the rest of the coarse-grained ureilitic lithologies. Both fragments have specific, unique textures: MS-153 contains beside olivine (~Fa_{10-12}) abundant pyroxene, whereas the olivine grains (~Fa_{15-17}) in MS-171 show some kind of lineation (Fig. 3f).

Two meteorite fragments are dominated by metals and sulfides. In one case such a **sulfide-metal assemblage** (MS-158; Fig. 4a) has an area of fine-grained ureilitic lithology attached (Fig. 4b). Highly reduced olivine is found in silicate inclusions within the sulfide-metal intergrowth. In a second fragment the sulfide-metal assemblage is very heterogeneous and porous (MS-166). One part is sulfide-rich (troilite) enclosing coarse-grained and fine-grained ureilitic olivine (Fig. 4c). The metal has about 17 wt% Ni. In another area of the fragment Si-poor metal with variable Ni-concentrations (about 7-20 wt%) is dominating (Fig. 4d). These metals are surrounded by small Ni-rich metal grains (~30 wt% Ni) and enclosed in a complicated intergrowth of small metals, Ni-bearing sulfides (probably troilites), and Fe-oxides (Fig. 4d).

Mineralogy - chondritic lithologies

From the 17 chondritic fragments identified, 14 belong to different enstatite chondrite types and two to the ordinary chondrite group. Among these chondritic varieties is also a unique chondrite – different to typical ordinary, carbonaceous, and Rumuruti (R) chondrites – which will be described in detail by Horstmann et al. (2010; this issue). Due to differences in texture, mineralogy, and mineral compositions the **14 enstatite chondrite** fragments represent at least seven different enstatite chondrites (EH3 (MS-14), EL3/4 (MS-17, MS-164), EL6 breccia (MS-D), EL6 (5 samples, Table 1), EL5/6 (MS-7, MS-159), EH5 (MS-155), shock-darkened EH4/5 (MS-13, MS-163) chondrites).

The two fragments of the **H-group ordinary chondrites** are different in mineralogy and texture: The H5 (MS-151) and H5/6 (MS-11; Fig. 5a) chondrites have different compositions of olivine and pyroxene (~$Fs_{17.5}$; ~$Fa_{20.5}$ and ~Fs_{14}; ~$Fa_{16.5}$, respectively). The fragment MS-151 is shock-darkened and the texture is barely visible in transmitted light. An even higher petrologic type cannot be ruled out.

The unique chondrite fragment (MS-CH) is a type 3.8±0.1 chondrite with a chondrule/matrix ratio of about 1.5 (Fig. 5b). Olivine is mainly Fa_{35-37}. Since the rock has a considerable abundance of mainly Ni-rich metal (Ni: ~40 wt%; Co: ~2 wt%) a relationship to CK and R chondrites (e.g., Kallemeyn et al., 1991; Geiger et al., 1993; Schulze et al., 1994;

Bischoff et al., 1994; Geiger and Bischoff, 1995) can be ruled out. For details see Horstmann et al. (2010).

In the following, some of the **enstatite chondrite** fragments will be characterized in more detail. The basic characteristics from the other fragments can be taken from Table 2. The Si-concentrations of metals in the EH and EL chondrites are distinctly different (Brearley and Jones, 1998). Within the EL group the Si content of kamacite increases from roughly 0.4 wt% in EL3s to 0.9-1.8 in EL5s and finally 1.1-1.7 in EL6s, whereas within the EH group the Si content of kamacite is about 2 wt% in EH3s increasing over 2.6-3.5 wt% in EH4s to roughly 4 wt% in EH6 chondrites (e.g., Keil, 1968; Sears et al., 1982; Brearley and Jones, 1998, and references therein). These criteria in combination with sulfide mineralogy and textural aspects were used to subdivide the E chondrites.

Almahata Sitta fragment MS-14 is a very unequilibrated EH3 chondrite (Fig. 3f), has highly variable compositions of low-Ca pyroxene ($Fs_{0.2-13}$; mean $Fs_{3\pm4}$), and contains minor forsteritic olivine. Preliminary data show that the abundant metals have mean Si-, Co-, and Ni-concentrations of approximately 3.1, 0.7, and 4.2 wt%, respectively. The Ni-concentrations vary from ~3 to ~7 wt%. Other phases include plagioclase, a SiO_2-phase, perryite, schreibersite, troilite, daubreelite, niningerite, and oldhamite.

Fragment MS-17 is an EL3/4-chondrite (Fig. 3d) having abundant chondrules. In some of these chondrules minor forsteritic olivine occurs. The enstatites contain low, but variable Fe-concentrations (Fs_{0-1}). Preliminary analyses show that the metals have Si-, Co-, and Ni-concentrations of about 0.5, 0.7, and 6.3 wt%, respectively. Other phases include Ca-pyroxene, plagioclase, a SiO_2-phase, graphite, troilite, oldhamite, and alabandite.

Some E chondrite fragments are shock-darkened. Fragment MS-13 is an EH4/5-chondrite (Fig. 3e), in which most enstatites have small, but significant Fs-contents (up to 1.6 mol%). The metals have Si-, Co-, and Ni-concentrations of roughly 2.7, 0.7, and 5.5 wt%, respectively. Other phases include plagioclase, a SiO_2-rich phase, troilite, niningerite, oldhamite, and graphite.

Seven samples are strongly metamorphosed EL chondrites. Five are classified as EL6 chondrites (Fig. 5f), one as an EL5/6, and the other one as a brecciated EL6 chondrite (see Fig. 1 in Horstmann and Bischoff, 2010). Some mineralogical information on these fragments is given in Table 2. The breccia MS-D is a highly recrystallized enstatite-rich rock which contains several clasts up to 5 mm in apparent size. Some of these clasts contain remarkably high abundances of Ca-pyroxene. The metals in MS-D have Si-, Co-, and Ni-concentrations of approximately 0.9, 0.5, and 5.5 wt%, respectively. Other yet identified phases include plagioclase, troilite, oldhamite, Zn-bearing alabandite, and keilite.

Oxygen isotope composition

The oxygen isotope compositions of 12 fragments (4 chondritic and 8 ureilitic) were determined (Table 5). All ureilite samples (MS-16, -20, -61, -124, -168, -169, -170 and -175) fall on the CCAM-line (Fig. 6). Three enstatite chondrite fragments (MS-52, -79, and -D) fall within uncertainty on the TFL in the enstatite chondrite field. Sample MS-151 was classified as H chondrite, but its oxygen isotope composition rather resembles that of R chondrites (Fig. 6). The oxygen isotope composition of fragment MS-CH will be discussed on Horstmann et al. (2010).

Cosmogenic radioisotopes

The measured activity concentrations for the detected cosmogenic radionuclides (^{22}Na, ^{54}Mn, ^{46}Sc, ^{26}Al, ^{57}Co, ^{60}Co) are given in Table 3. The detection of ^{46}Sc (half life: 83.8d) in MS-CH, and of ^{54}Mn (half life: 312.2d) and ^{57}Co (half life: 271.8d) in both samples clearly indicates that these fragments result from a very recent meteorite fall consistent with the Almahata Sitta fall. In particular the value for ^{46}Sc in MS-CH clearly indicates that this fragment results from a very recent meteorite fall, about 335 days to 420 days prior to the measurement. For the sample MS-D one can give only a much weaker estimate of the date of fall, using the ^{57}Co and the ^{54}Mn data. The range is 300 d to 600 d based on the available data in the literature for the measured activity concentrations for both radionuclides in chondrites (e.g., Evans et al., 1982). For the different values in ^{60}Co further analysis is needed in order to interpret the data correctly. The long-lived spallation product ^{26}Al has reached its saturation activity. The average production rate is well in agreement with the values cited in literature (Bhandari et al., 1993).

The activities measured for the isotopes ^{22}Na, ^{46}Sc, ^{57}Co and ^{54}Mn are in agreement with what is reported in literature for chondrites (Shedlovsky et al., 1967; Cressy, 1972; Mason, 1979; Evans et al., 1982).

The concentrations of the natural radionuclides ^{232}Th and ^{238}U as well as for K_{nat} in the meteorite specimens are listed in Table 4. They are well in accordance with the values reported in literature (Wasson and Kallemeyn, 1988).

Discussion:

A common asteroidal origin of chondritic and ureilitic lithologies in Almahata Sitta

We are convinced that most, if not all different lithologies described within this study belong to the Almahata Sitta meteorite fall. The main reasons can be summarized as follows: (a) The detection of the short and medium short-lived cosmogenic nuclides ^{46}Sc, ^{57}Co, and ^{54}Mn clearly indicates that the chondritic fragments MS-CH and MS-D result from a fresh meteorite fall consistent with the Almahata Sitta event in October, 2008. (b) Although most small fragments from the strewn field appear to represent fragments of a single lithology, preliminary studies show that at least some fragments contain two different lithologies (e.g., MS-124, MS-152, MS-158, MS-166). (c) Among the fragments at least 7 different E chondrite lithologies were detected. Enstatite chondrites are relatively rare (below 2 % of the actual meteorite flux) and such a high number of fresh E chondrite meteorite falls in just one small area can only be explained with a common origin in the asteroid 2008 TC_3. (d) The discovery of several new unique meteorite fragments (having so far unknown textures and mineralogy; e.g., MS-CH, MS-156, and MS-158) in a small area is only conceivable with a break-up of a polymict asteroid.

The ureilite fragments fall in the ureilite field in a 3-oxygen isotope diagram (Fig. 6). For the ureilite fragments, however, no systematic relation between Δ^{17}O and Fa-content of the olivine is observed (e.g., Mittlefehldt et al., 1998; compare Tables 1 and 5). The fine-grained ureilites cluster at high Δ^{17}O, whereas the coarse-grained ureilite fragments are more ^{16}O-rich (Fig. 6). The E chondrite fragments all fall within error on the TFL in the E chondrite field (Fig. 6) supporting the petrological classification.

The oxygen isotopes of fragment MS-151 do not agree with the petrographic classification as H chondrite. Instead, it resembles the composition of fragment MS-CH (see Horstmann et al., this issue), which is closely linked to R chondrites. The result illustrates that the Almahata Sitta breccia is fragmented on a very small scale and that the H and R chondrite-like lithologies may occurred in direct contact.

Mixing of different rock types in asteroids – fragments in chondrites

Studies on shock effects in meteorites and breccias are extremely important to reveal information on the evolution of asteroidal parent bodies (e.g., Bischoff et al., 1983, 2006; Bunch and Rajan, 1988; Stöffler et al., 1988, 1991; Bischoff and Stöffler, 1992). The existence and abundance of foreign and exotic fragments in meteorites give some measure of the degree of mixing among asteroids in the asteroidal belt. In addition, the relative abundance of different types of material in different meteorite breccias may tell something about the abundance of certain materials at different times and places in the asteroid belt. One of the most complicated meteorite breccias is Kaidun (Zolensky and Ivanov, 2003), which will be described below; however, only a few meteorites contain more than a few volume percent of foreign clasts and the most abundant clasts are CM-like chondritic fragments (Meibom and Clark, 1999; Bischoff et al., 2006).

In ordinary chondrite breccias, fragments from other ordinary chondrite groups are very rare and are summarized in Bischoff et al. (2006). These include: (a) intensely shocked H-group chondrite fragments in the LL chondrite St. Mesmin (Dodd, 1974); (b) an LL5 clast in the Dimmitt H chondrite regolith breccia (Rubin et al., 1983); (c) an L-group melt rock fragment in the LL chondrite Paragould (Fodor and Keil, 1978); (d) fragments in Adzhi-Bogdo (LL3-6), which appear to derive from L-group chondrites (Bischoff et al., 1993, 1996); (e) a troctolitic clast with an H-chondrite oxygen isotopic composition in the Y-794046 (L6) chondrite (Prinz et al., 1984); (f) an L-chondritic inclusion in the Fayetteville H-chondrite regolith breccia (Wieler et al., 1989); and (h) a fragment of H chondrite parentage within the Ngawi LL chondrite (Fodor and Keil, 1975).

CM-type fragments occur in different groups of chondrites: A small CM chondrite clast with a matrix of phyllosilicates and sulfide was observed in the Magombedze (H3-5) chondrite breccia (MacPherson et al., 1993). In addition, a carbonaceous clast was found in the H-group ordinary chondrite breccia Dimmitt (Rubin et al., 1983) and other possible carbonaceous clasts in various ordinary chondrites are given by Keil (1982).

In addition, some differentiated, achondritic clasts were recorded from brecciated chondrites (e.g., Hutchison et al., 1988; Fredriksson et al., 1989; Bridges and Hutchison, 1997; Bischoff et al., 1993, 2006; Sokol et al., 2007a,b; Terada and Bischoff, 2009).

Mixing of different rock types in asteroids – fragments in achondrites

From several polymict HED breccias (e.g., Kapoeta and LEW 85300) Wilkening (1973) and Zolensky et al. (1992, 1996) report on carbonaceous chondrite clasts, mineralogically similar to CM and CV3 chondrites. The occurrence of other chondritic clasts in brecciated HED achondrites was further reported by Bunch et al. (1979), Kozul and Hewins (1988), Mittlefehldt and Lindstrom (1988), Hewins (1990), Reid et al. (1990), Buchanan et al. (1993), Mittlefehldt (1994), Pun et al. (1998), and Buchanan and Mittlefehldt (2003).

In polymict ureilites ordinary chondrite fragments have been found (e.g., Jaques and Fitzgerald, 1982; Prinz et al., 1986, 1987, 1988; Ikeda et al., 2000, 2003; Ross et al., 2010) and angrite-like clasts were reported from several meteorites (e.g., Jaques and Fitzgerald, 1982; Prinz et al., 1986, 1987; Ikeda et al., 2000; Goodrich and Keil, 2002; Cohen et al., 2004; Kita et al., 2004). Fine-grained dark clasts mineralogically similar to fine-grained carbonaceous chondrite material are also known to exist in some ureilites (e.g., Prinz et al., 1987; Brearley and Prinz, 1992; Ikeda et al., 2000, 2003; Goodrich and Keil, 2002). Recently, some ureilites having impact-molten areas were identified indicating severe melting and mixing on the ureilite parent body (Warren and Rubin, 2006; Janots et al., 2009, 2010). The previous finding of the mixing of chondritic and ureilitic components is an important aspect to consider the mineralogical and lithological behaviour of asteroid 2008 TC_3 studied here.

Formation of asteroid 2008 TC_3

Bischoff et al. (2006) concluded that "asteroids are generally modified by two kinds of hypervelocity impacts: frequent impacts that crater the surface, and large rare impacts that damage the whole asteroid and create large volumes of rubble". A mayor fraction of meteorite breccias is created by these large impacts (e.g., Scott, 2002; Scott and Wilson, 2005). Meteorites containing foreign clasts are typically regolith breccias, but the absence of solar wind gases excludes the possibility that Almahata Sitta is a regolith breccia (Ott et al., 2010). As shown in this paper Almahata Sitta has at least 10 different ureilitic lithologies and at least further 10 different – in one case unique (Horstmann et al., 2010) – chondritic rock types. Considering the 10 ureilitic lithologies and their extraordinary diversity alone, it is clear that the coexistence of these lithologies in Almahata Sitta can only be the result of a gigantic and catastrophic disruption and breakup of the ureilite parent body delivering and producing all these different ureilitic lithologies. At the same time all sorts of chondritic fragments must have been present in a debris disk around the sun. The chondritic and ureilitic components were mixed and accreted to form asteroid 2008 TC_3. From the study of Almahata Sitta fragments we have no information about the presence of primordial dust in the region of reaccretion. Since most of the studied fragments consist of a single lithology, we suggest that the highly porous, fine-grained ureilite material described in Almahata Sitta by Jenniskens et al. (2009) may represent only the weak and relatively unconsolidated matrix (probably of low modal abundance) which surrounded the monolithic clasts. Our studied small fragments – especially the chondritic ones - are not porous and are presumably not inherently weak. Considering the Almahata Sitta bulk rock in general, we have no information on the strength and lithological connections of the various chondritic and achondritic components in Almahata Sitta. However, we suggest that Almahata Sitta was much more loosely lithified and porous than Kaidun (Zolenskly and Ivanov, 2003), which is a well consolidated breccia, in which the relationship between different lithologies can be studied in much more detail than in the case of Almahata Sitta.

Kaidun – probably the closest analog to Almahata Sitta

The Kaidun breccia basically consists of chondritic components and not of achondritic constituents. But, based on the huge variety of different types of chondritic fragments we suggest that Kaidun is the closest analog of Almahata Sitta. Based on the exceptional variety of rock-types, Zolensky and Ivanov (2003) characterized the Kaidun microbreccia as a "harvest from the inner and outer asteroid belt". Kaidun consists almost entirely of millimeter and sub-millimeter-sized fragments of EH3-5, EL3, CV3, CM1-2, and R chondrites (Ivanov, 1989; Ivanov et al., 2003; Zolensky and Ivanov, 2003, and references therein), contains C1 and C2 lithologies, fragments of impact melt products, new enstatite-bearing clasts, phosphide-bearing fragments, clasts of Ca-rich achondrite, possibly aubritic materials, and alkaline-enriched clasts, (Ivanov, 1989; Ivanov et al., 2003; Zolensky and Ivanov, 2003; Kurat et al., 2004). The alkaline-enriched clasts are similar to the granitoidal clasts found in the Adzhi-Bogdo ordinary chondrite regolith breccia (Bischoff et al., 1993, 1996; Sokol and Bischoff, 2006; Sokol et al., 2007a,b; Terada and Bischoff, 2009). In addition, a possible ordinary chondrite clast has been characterized by Mikouchi et al. (2005). Thus, after the polymict breccia Kaidun (Zolensky and Ivanov, 2003) Almahata Sitta is a new extraordinary breccia for future studies.

The mismatch in reflectance spectra

Based on Gaffey et al. (1993) ureilites should derive from S-type asteroids. These authors distinguish between pyroxene-poor ureilites (class S(I)), clinopyroxene-bearing ureilites (class S(II)), clinopyroxene and orthopyroxene-bearing ureilites (class S(III)), and orthopyroxene-bearing ureilites (class S(IV)). However, the reflectance spectra of asteroid 2008 TC_3 are similar to those of B- and F-type asteroids (Jenniskens et al., 2009). Based on Gaffey et al. (1993) type B asteroids should contain iron-poor hydrated silicates and type F asteroids should have hydrated silicates and organics. Jenniskens et al. (2009) did not find hydrated silicates in the Almahata Sitta meteorite sample, but came to the somewhat surprising conclusion that Almahata Sitta is similar to a type F asteroid. The asteroid 2008 TC_3 analyzed in space was a mixture of very different lithologies. It is not certain, if all different lithologies have been recognized so far: This is probably not the case. Perhaps, also lithologies with hydrated silicates existed within the asteroid 2008 TC_3. Based on the findings presented in this paper the reflectance spectrum of asteroid 2008 TC_3 has to be evaluated in a new light.

Acknowledgements: We thank U. Heitmann (Münster) for sample preparation. N. Albrecht (Göttingen) is thanked for the preparation of the oxygen isotope analyses and Ed Scott (University of Hawaii) for interesting discussions on the possible accretion scenario of asteroid 2008 TC_3.

References:

Bhandari N., Mathew K. J, Rao M. N., Herpers U., Bremer K., Vogt S., Wölfli W., Hofmann, H. J., Michel R., Bodemann R., and Lange H.-J. 1993. Depth and size dependence of cosmogenic nuclide production rates in stony meteoroids. *Geochimica et Comochimica Acta* 57:2361-2375.

Bischoff A. and Stöffler D. 1992. Shock metamorphism as a fundamental process in the evolution of planetary bodies: Information from meteorites. *European Journal of Mineralogy* 4:707-755.

Bischoff A., Rubin A. E., Keil K., and Stöffler D. 1983. Lithification of gas-rich chondrite regolith breccias by grain boundary and localized shock melting. *Earth and Planetary Science Letters* 66:1-10.

Bischoff A., Geiger T., Palme H., Spettel B., Schultz L., Scherer P., Schlüter J., and Lkhamsuren J. 1993. Mineralogy, chemistry, and noble gas contents of Adzhi-Bogdo – an LL3-6 chondritic breccia with L-chondritic and granitoidal clasts. *Meteoritics* 28:570-578.

Bischoff A., Geiger T., Palme H., Spettel B., Schultz L., Scherer P., Loeken T., Bland P., Clayton R. N., Mayeda T. K., Herpers U., Meltzow B., Michel R., and Dittrich-Hannen B. 1994. Acfer 217 - A new member of the Rumuruti chondrite group (R). *Meteoritics* 29:264-274.

Bischoff A., Gerel O., Buchwald V. F., Spettel B., Loeken T., Schultz L., Weber H. W., Schlüter J., Baljinnyam L., Borchuluun D., Byambaa C., and Garamjav D. 1996. Meteorites from Mongolia. *Meteoritics & Planetary Science* 31:152-157.

Bischoff A., Scott E. R. D., Metzler K., and Goodrich C. A. 2006. Nature and Origins of meteoritic breccias. In Meteorites and the Early Solar System II, edited by Lauretta D.S. and McSween Jr. H.Y. Tucson: University of Arizona Press. pp. 679-712.

Bischoff A., Horstmann M., Laubenstein, M., and Haberer S. 2010. Asteroid 2008 TC_3 – Almahata Sitta: Not only a ureilitic meteorite, but a breccia containing many different achondritic and chondritic lithologies (abstract #1763). 41st Lunar and Planetary Science Conference.

Brearley A. J. and Jones R. H. 1998. Chondritic meteorites. In *Planetary Materials – Reviews in Mineralogy*, Vol. 26, edited by Papike J.J. Mineralogical Society of America, pp.3-01 – 3-398.

Brearley A. J. and Prinz M. 1992. CI chondrite-like clasts in the Nilpena polymict ureilite. Implications for aqueous alteration processes in CI chondrites. *Geochimica et Cosmochimica Acta* 56:1373-1386.

Bridges J. C. and Hutchison R. 1997. A survey of clasts and chondrules in ordinary chondrites. *Meteoritics & Planetary Science* 32:389–394.

Buchanan P. C. and Mittlefehldt D. W. 2003. Lithic components in the paired howardites EET 87503 and EET 87513: Characterization of the regolith of 4 Vesta. *Antarctic Meteorite Research* 16:128-151.

Buchanan P. C., Zolensky M. E., and Reid A. M. 1993. Carbonaceous chondrite clasts in the howardites Bholghati and EET87513. *Meteoritics* 28:659-669.

Bunch T. E. and Rajan R. S. 1988. Meteorite regolith breccias. In *Meteorites and the Early Solar System*, edited by Kerridge J. F. and Matthews M. S. Tuscon: The University of Arizona Press. pp. 144-164.

Bunch T. E., Chang S., Frick U., Neil J. and Moreland G. 1979. Carbonaceous chondrites - I. Characterisation and significance of carbonaceous chondrite (CM) xenoliths in the Jodzie howardite. *Geochimica et Cosmochimica Acta* 43:1727-1742.

Cohen B. A., Goodrich C. A., and Keil K. 2004. Feldspathic clast populations in polymict ureilites: Stalking the missing basalts from the ureilite parent body. *Geochimica et Cosmochimica Acta* 68:4249-4266.

Cressy, P. J. Jr. 1972. Cosmogenic radionuclides in the Allende and Murchison carbonaceous chondrites. *Journal of Geophysical Research* 77:4905–4911.

Dodd R. T. 1974. Petrology of the St. Mesmin chondrite. *Contributions to Mineralogy and Petrology* 46:129-145.

Evans, J. C., Reeves, J. H., Rancitelli, L. A. and Bogard, D. D. 1982. Cosmogenic nuclides in recently fallen meteorites: Evidence for galactic cosmic ray variations during the period 1967–1978. *Journal of Geophysical Research* 87:5577–5591.

Fodor R. V. and Keil K. 1975. Implications of poikilitic textures in LL-group chondrites. *Meteoritics* 10:325-340.

Fodor R. V. and Keil K. 1978. Catalog of lithic fragments in LL-Group chondrites. *Special Publication No.* 19, University of New Mexico, Institute of Meteoritics, pp. 38.

Fredriksson K., Jarosewich E., and Wlotzka F. 1989. Study Butte: A chaotic chondrite breccia with normal H-group chemistry. *Zeitschrift für Naturforschung* 44a:945–962.

Gaffey M. J., Burbine T. H., and Binzel R. P. 1993. Asteroid spectroscopy: Progress and perspectives. *Meteoritics* 28:161-187.

Geiger T. and Bischoff A. 1995. Formation of opaque minerals in CK chondrites. *Planetary and Space Science* 43:485-498.

Geiger T., Spettel B., Clayton R. N., Mayeda T. K., and Bischoff A. 1993. Watson 002 - the first CK - type 3 chondrite. *Meteoritics* 28:352.

Goodrich C. A. and Keil K. 2002. Feldspathic and other unusual clasts in polymict ureilite DaG 165 (abstract #1777). 33rd Lunar and Planetary Science Conference.

Herrin J. S., Zolensky M. E., Ito M., Jenniskens P., Shaddad M. H. 2009. Fossilized smelting: Reduction textures in Almahata Sitta ureilite (abstract). *Meteoritics & Planetetary Science* 44:A89.

Hewins R.H. 1990. Geologic history of LEW 85300, 85302 and 85303 polymict eucrites (abstract). 21st Lunar and Planetary Science Conference 21:509-510.

Horstmann M. and Bischoff A. 2010. Characterization of spectacular lithologies from the Almahata Sitta breccia (abstract #1784). 41st Lunar and Planetary Science Conference.

Horstmann M., Bischoff A., Pack A., and Laubenstein M. 2010. Almahata Sitta – fragment MS-CH: Characterization of a new chondrite type. *Meteoritics & Planetary Science* 45, this issue.

Hutchison R., Williams C. T., Din V. K., Clayton R. N., Kirschbaum C., Paul R. L., and Lipschutz M. E. 1988. A planetary, H-group pebble in the Barwell, L6, unshocked chondritic meteorite. *Earth and Planetary Science Letters* 90:105–118.

Ikeda Y., Prinz M., and Nehru C. E. 2000. Lithic and mineral clasts in the Dar al Gani (DAG) 319 polymict ureilite. *Antarctic Meteorite Research* 13:177-221.

Ikeda Y., Kita N. T., Morishita Y., and Weisberg M. K. 2003. Primitive clasts in the Dar al Gani 319 polymict ureilite: Precursors of the ureilites. *Antarctic Meteorite Research* 16:105-127.

Ivanov A. V. 1989. The Kaidun meteorite: composition and history. *Geochemistry International* 26:84-91.

Ivanov A. V., Kononkova N. N., Yang A. V., and Zolensky M. E. 2003. The Kaidun meteorite: Clasts of alkaline-rich fractionated materials. *Meteoritics & Planetary Science* 38:725-737.

Janots E., Gnos E., Hofmann B. A., Greenwood R. C., Franchi I. A., and Bischoff A. 2009. Jiddat al Harasis 422: The first ureilitic impact melt breccia (abstract). *Meteoritics & Planetary Science* 44:A100.

Janots E., Gnos E., Hofmann B. A., Greenwood R. C., Franchi I. A., and Bischoff A. 2010. Jiddat al Harasis 422: the strongest shock-melted ureilite. *Meteoritics & Planetary Science* (submitted).

Jaques A. L. and Fitzgerald M. J. 1982. The Nilpena ureilites, an unusual polymict breccia: implications for origin. *Geochimica et Cosmochimica Acta* 46:893-900.

Jenniskens P., Shaddad M. H., Numan D., Elsir S., Kudoda A. M., Zolensky M. E., Le L., Robinson G. A., Friedrich J. M., Rumble D., Steele A., Chesley S. R., Fitzsimmons A., Duddy S., Hsieh H. H., Ramsay G., Brown P. G., Edwards W. N., Tagliaferri E., Boslough M. B., Spalding R. E., Dantowitz R., Kozubal M., Pravec P., Borovicka J., Charvat Z., Vaubaillon J., Kuiper J., Albers J., Bishop J. L., Mancinelli R. L., Sandford S. A., Milam S. N., Nuevo M., and Worden S. P. 2009. The impact and recovery of asteroid 2008 TC_3. *Nature* 458:485-488.

Kallemeyn G. W., Rubin A. E., and Wasson J. T. 1991. The compositional classification of chondrites: V. The Karoonda (CK) group of carbonaceous chondrites. *Geochimica et Cosmochimica Acta* 55:881-892.

Keil K. 1968. Mineralogical and chemical relationships among enstatite chondrites. *Journal of Geophysical Research* 73:6945-6976.

Keil K. 1982. Composition and origin of chondritic breccias. In *Workshop on Lunar Breccias and Soils and Their meteoritic Analogs*, LPI Technical Report 82-02, edited by Taylor G. J. and Wilkening L. L.: Lunar Planetary Institute. pp. 65-83.

Kita N. T., Ikeda Y., Togashi S., Liu Y., Morishita Y., and Weisberg M. K. 2004. Origin of ureilites inferred from a SIMS oxygen isotopic and trace element study of clasts in the Dar al Gani 319 polymict ureilite. *Geochimica et Cosmochimica Acta* 68:4213-4235.

Kozul J. and Hewins R.H. 1988. LEW 85300,02,03 polymict eucrites consortium – II: Breccia clasts, CM inclusions, glassy matrix and assembly history (abstract). 19th Lunar and Planetary Science Conference 19:647-648.

Kurat G., Zinner E., Brandstätter F., and Ivanov A. V. 2004. Enstatite aggregates with niningerite, heideite, and oldhamite from the Kaidun carbonaceous chondrite: Relatives of aubrites and EH chondrites ?. *Meteoritics & Planetary Science* 39:53-60.

MacPherson G. J., Jarosewich E., and Lowenstein P. 1993. Magombedze: A new H-chondrite with light-dark structure. *Meteoritics* 28:138-142.

Mason, B. 1979. Meteorites. In *Data of Geochemistry*, 6th ed., Chapter B, Cosmochemistry, Part 1., edited by Fleischer M. Geological Survey Professional Paper 440-B-1. pp. B1–B132.

Meibom A. and Clark B. E. 1999. Evidence for the insignificance of ordinary chondrite material in the asteroid belt. *Meteoritics & Planetary Science* 34:7-24.

Mikouchi T., Makishima J., Koizumi E., and Zolensky M. E. 2005. Porphyritic olivine-pyroxene clast in Kaidun: First discovery of an ordinary chondrite clast? (abstract #1956). 36th Lunar and Planetary Science Conference.

Mittlefehldt D. W. 1994. The genesis of diogenites and HED parent body petrogenesis. *Geochimica et Cosmochimica Acta* 58:1537-1552.

Mittlefehldt D. W. and Lindstrom M. M. 1988. Geochemistry of diverse lithologies in antarctic eucrites (abstract). 19th Lunar and Planetary Science Conference 19:790-791.

Mittlefehldt D. W., McCoy T. J., Goodrich C. A., and Kracher A. 1998. Non-chondritic meteorites from the asteroidal belt. In *Planetary Materials – Reviews in Mineralogy*, Vol. 26, edited by Papike J. J., Mineralogical Society of America. pp. 4-01 – 4-170.

Ott U., Herrmann S., Jenniskens P. M., and Shaddad M. 2010. A noble gas study of two stones from the Almahata Sitta meteorite. (abstract #1195). 41st Lunar and Planetary Science Conference. CD-ROM.

Prinz M., Nehru C. E., Weisberg M. K., Delany J. S., Yanai K., and Kojima H. 1984. H-chondritic clasts in a Yamato L6 chondrite: Implications for metamorphism. *Meteoritics* 19:292-293.

Prinz M., Weisberg M. K., Nehru C. E., and Delaney J. S. 1986. North Haig and Nilpena: Paired polymict ureilites with Angra dos Reis-related and other clasts (abstract). 17th Lunar and Planetary Science Conference 17:681-682.

Prinz M., Weisberg M. K., Nehru C. E., and Delaney J. S. 1987. EET83309, a polymict ureilite: Recognition of a new group (abstract). 18th Lunar and Planetary Science Conference 18:802-803.

Prinz M., Weisberg M. K., and Nehru C. E. 1988. Feldspathic components in polymict ureilites (abstract). 19th Lunar and Planetary Science Conference 19:947-948.

Pun A., Keil K., Taylor G.J. and Wieler R. 1998. The Kapoeta howardite: Implications for the regolith evolution of the howardite-eucrite-diogenite parent body. *Meteoritics & Planetary Science* 33:835-851.

Reid A. M., Buchanan P., Zolensky M. E. and Barrett R. A. 1990. The Bholghati howardite: petrography and mineral chemistry. *Geochimica et Cosmochimica Acta* 54:2161-2166.

Ross A. J., Downes H., Smith C. S., and Jones A. P. 2010. DaG 1047: A polymict ureilite containing exotic clasts including a chondrites (abstract #2361). 41st Lunar and Planetary Science Conference.

Rubin A. E., Scott E. R. D., Taylor G. J., Keil K., Allen, J. S. B., Mayeda T. K., Clayton R. N., and Bogard D. D. 1983. Nature of the H chondrite parent body regolith: Evidence from the Dimmitt breccia. Proceedings. 13th Lunar and Planetary Science Conference. pp. A741-A754.

Schulze H., Bischoff A., Palme H., Spettel B., Dreibus G., and Otto J. 1994. Mineralogy and chemistry of Rumuruti: The first meteorite fall of the new R chondrite group. *Meteoritics* 29:275-286.

Scott E. R. D. 2002. Meteorite evidence for the accretion and collisional evolution of asteroids. In *Asteroids III* (W. F. Bottke et al., eds.) pp. 697-709. Univ. of Arizona, Tucson

Scott E. R. D. and Wilson L. 2005. Meteoritic and other constraints on the internal structure and impact history of small asteroids. *Icarus*, 74:46-63.

Sears D. W., Kallemeyn G. W., and Wasson J. T. 1982. The compositional classification of chondrites: II The enstatite chondrites groups. *Geochimica et Cosmochimica Acta* 46: 597-608.

Shedlovsky J. P., Cressy P. J. Jr. and Kohman T. P. 1967. Cosmogenic radioactivities, in the Peace River and Harleton chondrites. *Journal of Geophysical Research* 72:5051–5058.

Sokol A. K. and Bischoff A. 2006. Simultaneous accretion of differentiated or metamorphosed asteroidal clasts and chondrules (abstract). *Meteoritics & Planetary Science* 41:A164.

Sokol A. K., Bischoff A., Marhas K. K., Mezger K., and Zinner E. 2007a. Simultaneous accretion of differentiated or metamorphosed asteroidal clasts and chondrules (abstract). *Meteoritics & Planetary Science* 42:A143.

Sokol A. K., Bischoff A., Marhas K. K., Mezger K., and Zinner E. 2007b. Late accretion and lithification of chondritic parent bodies: Mg isotope studies on fragments from primitive chondrites and chondritic breccias. *Meteoritics & Planetary Science* 42:1291-1308.

Stöffler D., Bischoff A., Buchwald V., and Rubin A. E. 1988. Shock effects in meteorites. In *Meteorites and the Early Solar System*, edited by Kerridge J. F. and Matthews M. S. Tuscon: The University of Arizona Press. pp. 165-202.

Stöffler D., Keil K., and Scott E. R. D. 1991. Shock metamorphism of ordinary chondrites. *Geochimica et Cosmochimica Acta* 55:3845-3867.

Terada K. and Bischoff A. 2009. Asteroidal granite-like magmatism 4.53 Gyr ago. *The Astrophysical Journal* 699:L68-L71.

Warren P. H. and Rubin A. E. 2006. Melted-reduced pigeonite, vermicular silica, sirich glasses, and other impact-smelting products in the LAR 04315 ureilite (abstract). *Meteoritics & Planetary Science* 41:A184.

Wasson J. T. and Kallemeyn G. W. 1988. Compositions of Chondrites. *Philosophical Transactions of the Royal Society of London.* Series A, Mathematical and Physical Sciences, The Solar System: Chemistry as a Key to Its Origin, Vol. 325, 1587:535-545.

Weber I., Bischoff A., and Weber D. 2003. TEM investigations on the monomict ureilites Jalanash and Hammadah al Hamra 064. *Meteoritics & Planetary Science* 38:145-156.

Wieler R., Graf T., Pedroni A., Signer P., Pellas P., Fieni C., Suter M., Vogt S., Clayton R. N., and Laul J. C. 1989. Exposure history of the regolithic chondrite Fayetteville: II. Solar-gas-free light inclusions. *Geochimica et Cosmochimica Acta* 53:1449-1459.

Wilkening L. L. 1973. Foreign inclusions in stony meteorites – I. Carbonaceous chondritic xenoliths in the Kapoeta howardite. *Geochimica et Cosmochimica Acta* 37:1985-1989.

Zolensky M. and Ivanov A. 2003. The Kaidun microbreccia meteorite: A harvest from the inner and outer asteroid belt. *Chemie der Erde - Geochemistry* 63:185-246.

Zolensky M. E., Hewins R. H., Mittlefehldt D. W., Lindstrom M. M., Xiao X., and Lipschutz M. E. 1992. Mineralogy, petrology and geochemistry of carbonaceous chondritic clasts in the LEW 85300 polymict eucrite. *Meteoritics* 27:596-604.

Zolensky M. E., Weisberg M. K., Buchanan P. C., and Mittlefehldt D. W. 1996. Mineralogy of carbonaceous chondrite clasts in HED achondrites and the moon. *Meteoritics & Planetary Science* 31:518-537.

Zolensky M. E., Herrin J., Jenniskens P., Friedrich J. M., Rumble D., Steele A., Sandford S. A., Shaddad M. H., Le L., Robinson G. A., and Morris R. V. 2009. Mineralogy of the Almahata Sitta ureilite (abstract). *Meteoritics & Planetary Science* 44:A227.

Table 1. Ureilitic lithologies in the Almahata Sitta meteorite.

Frag-No.	Frag. mass	Typical grain size*	Olivine cores (Fa)	Range (Fa)	Pyroxene cores (Fs)	Range (Fs)	Comments
Coarse-grained ureilitic fragments							
MS-16	4.31g	500-800	5-6	2-6	5-6	5-6	px-dominating; 4-5 wt% Ni in metal; ureilitic?
MS-153	7.43g	100-300 µm	10-12	8-13	10-11.5		pyroxene-rich
MS-156	16,00g	>1 mm	17-19	4-19	11-12.5	4-12.5	
MS-157	3.68g	0.8-1.2 mm	12-13	2-13	10-11	2-11	
MS-160	8.39g	>1 mm	17-19	1-19			pyroxene-poor
MS-162	4.74g	400-600 µm	16-18	1.5-18	6-7	2-7	grains up to 2.5 mm
MS-167	49.14g	0.6-1.5 mm	20.5-22	2-22	17-18.5	1-18.5	
MS-169	26.29g	300-600 µm	11-12.5	1-12.5	10.5-11	0.5-11	pyroxene-rich
MS-170	26.81g	400-800 µm	20-22	1-22	17-19	3-19	
MS-171	34.35g	100-300 µm	15-16.5	5-16.5	12-14	9-14	variable grain size
MS-173	32.30g	0.8-1.2 mm	11.5-13.5	6-13.5	10.5-11.5	0.5-11.5	pyroxene-rich
MS-175	7.46g	300-600 µm	10-12	2-12	8-10	2-10	pyroxene-rich
Fine-grained ureilitic fragments							
MS-20	3.55g	<30 µm	8-9	0-9	10-12	0-12	metal-rich areas with niningerite
MS-28	37.92g	<20 µm	11-13	3-13	11-13	2-13	
MS-61	16.55g	<20 µm	mean: 13.5±3.6	mainly 11-17	mean: 11.7±2.5	3-17	
MS-124	34.02	mostly: <20 µm	19-21	3-21	16-18	1-18	contains coarser-grained fragment
MS-152	9.13g	<30 µm	mainly: 12-14	3-18	14-16	7-16	Reduced fragment: ~Fa_1
MS-154	4.18g	<20 µm	mean: 3.6	0-8	6-8	1.5-8	
MS-161	4.88g	<30 µm	18-19.5	1-19.5	14.5-15.5	12-15.5	suessite
MS-165	2.63g	<20 µm	15-18	2.5-18	12-14	0-14	area with niningerite
MS-168	33.18g	<20 µm	mainly: 0-8	0-21	mean: 4.8±4	0-14	area with 18-20.5 mol% Fa
Metal-sulfide dominating fragments with enclosed ureilitic portions							
MS-158	9.05g	<20 µm	17-20	10-20	not analyzed		data for the fine-grained portion
MS-166	3.25g	up to 120 µm	12-14	2-14	13-15	2-15	coarse-grained ol inclusion; Ni-rich metals

*) for the coarse-grained ureilitic fragments the grain size determination can only be a rough estimate, because of the limited sample size. In some cases only a few grains were available.

Table 2. Chondritic lithologies in the Almahata Sitta meteorite.

Frag-No.	Frag. mass	Class	Fa	Fs	Fs (range)	sulfides	Ni in met. (wt%)	Si in met. (wt%)	Comments
MS-D	17.34g	EL6		<0.3		oldhamite, troilite, keilite, Zn-alabandite	5.5	0.9	breccia
MS-CH	5.68g	unique	mainly: 35-37	14.4±7.5	3-26	troilite	mainly:~40; Co:~2	<0.2	Fa range: 19-38; matrix: ~45 vol%
MS-7	8.73g	EL5/6		<0.3		oldhamite, troilite, alabandite	6.9	0.8	
MS-11	6.88g	H5/6	16.5	14		troilite	7.6	<0.2	Co in metal: 0.8
MS-13	5.02g	EH4/5		0.6±0.4	0-1.6	oldhamite, troilite, niningerite	5.5	2.7	shock-darkened
MS-14	4.69g	EH3		2.9±3.7	0-13	oldhamite, troilite, daubreelite, niningerite	4.2 (3.2-6.5)	3.1	perryite
MS-17	4.22g	EL3/4	0.2 (1 grain)	0.5±0.3	0-1	oldhamite, alabandite, troilite	6.3	0.5	
MS-52	18.17g	EL6		<0.3		troilite, oldhamite, alabandite	6.4	0.9	
MS-79	14.71g	EL6		<0.4		troilite, oldhamite, alabandite	6.4	0.9	
MS-150	25.46g	EL6		<0.3		oldhamite, troilite, alabandite	6.3	1.5	schreibersite
MS-151	4.78g	H5	20.5	17.7		troilite	8.2	<0.1	Co in metal: 0.7 wt%; shock-darkened
MS-155	3.11g	EH5		0.38±0.2		oldhamite, troilite, niningerite	5.6	3.3	
MS-159	4.23g	EL5/6		0.4±0.3		oldhamite, troilite, keilite	5.6	0.8	
MS-163	9.94g	EH4/5		1.1±0.55	0.1-1.9	troilite, keilite, niningerite	6.5	3.3	shock-darkened
MS-164	8.90g	EL3/4		0.4±0.5	0-2	oldhamite, troilite	5.6	1.4	schreibersite
MS-172	45.52g	EL6		<0.3		troilite, alabandite, oldhamite	6.5	1.2	
MS-174	12.24g	EL6		<0.3		troilite, oldhamite, alabandite	6.3	0.8	

Table 3: Data summary for the detected cosmogenic radionuclides in two samples of the Almahata Sitta meteorite. The reported uncertainties in the last digits (in parentheses) are expanded uncertainties with k=1, the upper limits are given with 90% C.L. For data on MS-CH see also Horstmann et al. (2010).

radionuclide	half-life	Activity concentrations in [dpm kg^{-1}]	
		MS-CH (5.1 g)	MS-D (8.65 g)
^{26}Al	717000 y	57 (12)	75 (8)
^{60}Co	5.2710 y	22 (5)	84 (6)
^{54}Mn	312.13 d	114 (19)	134 (14)
^{22}Na	2.6027 y	78 (15)	104 (12)
^{46}Sc	83.788 d	19 (8)	< 22
^{57}Co	271.8 d	22 (10)	16 (3)

Table 4: Results for the naturally occurring nuclides Th, U, and K_{nat} in two samples of the Almahata Sitta meteorite. The reported uncertainties in the last digits (in parentheses) are expanded uncertainties with k=1, the upper limits are given with 90% C.L.

nuclide	concentrations in [ng g^{-1}]	
	MS-CH	MS-D
	(5.1 g)	(8.65 g)
Th	< 40	20 (7)
U	38 (14)	5 (2)
K_{nat}	$635 (100) \times 10^3$	$632 (66) \times 10^3$

Table 5: Oxygen isotope composition of Almahata Sitta fragments. Data are reported in ‰ relative to SMOW. *) mean, see Horstmann et al. (2010) for details.

Sample	$\delta^{17}O$	$\delta^{18}O$	$\Delta^{17}O$
MS-16	2.28	6.28	-1.05
MS-169	1.55	6.16	-1.69
MS-170	3.40	7.97	-0.82
MS-175	2.97	7.30	-0.89
MS-20	3.99	7.99	-0.23
MS-61	3.57	7.94	-0.60
MS-124	3.42	7.59	-0.59
MS-168	3.80	8.10	-0.48
MS-D	3.06	5.85	-0.01
MS-52	3.31	6.27	0.02
MS-79	3.31	6.17	0.07
MS-151	4.82	6.46	1.40
MS-CH*	4.94	4.33	1.73

Figure Captions:

Fig. 1: Fine-grained ureilitic lithologies in Almahata Sitta: (a) MS-161 – typical fine-grained ureilitic lithology (polarized light, crossed polarizers); (b) MS-152 – fine-grained lithology with a reduced clast (polarized light, crossed polarizers); (c) MS-125 – this fine-grained fragment has a coarser-grained ureilitic fragment (polarized light, crossed polarizers); (d) MS-165 - reflected light photomicrograph of a niningerite-bearing, metal-rich area within the fine-grained ureilitic fragment. FeS = Cr-bearing troilite; K = Kamacite; (e) MS-20 – metal- and sulfide-rich area of the fine-grained ureilitic fragment having niningerite, troilite, and remarkable concentrations of Si and Ni in kamacite (K); reflected light; (f) MS-168: Low-Ca pyroxene (Px) often occurs intergrown with olivine (Ol), Ca-pyroxene (Cpx), and troilite (FeS) within the fine-grained ureilitic lithology. Ca-pyroxene is mostly an interstitial phase. The tiny white particles are mainly FeS, only some are kamacite (K). P = pores; backscattered electron (BSE) image.

Fig. 2: Different varieties of coarse-grained ureilitic lithologies. (a) MS-160 and (b) MS-167: Typical ureilitic lithology with abundant olivine; (c) and (d) MS-175 (similar area in both images): This type of coarse-grained fragments can be characterized in having abundant pyroxene (most of the grey to dark-grey grains in (c)). Grain boundaries are visible based on the distribution of metals and sulfides (white). Photomicrographs were taken in polarized light, crossed polarizers, except the BSE-image (d).

Fig. 3: (a) MS-169 is a coarse-grained fragment having abundant pyroxene; (b) MS-16: Pyroxene-dominating rock; (c) MS-156: A unique type of ureilitic lithology with an internal texture (d) showing zoned olivine (~Fa_{8-19}) and a sulfide/metal network; (e) MS-153 and (f) MS-171: These fragments have a smaller grain size than the other coarse-grained ureilitic lithologies. Ol = olivine, Fa = fayalite, Px = pyroxene. All photomicrographs were taken in polarized light, crossed polarizers, except for the backscattered electron image of (d).

Fig. 4: Fragments dominated by metal-sulfide assemblages. (a) The sulfide-metal portion of fragment MS-158 includes highly reduced olivines in the silicate-rich areas (grey). Holes are black (P); (b) fine-grained ureilitic portion attached to the metal-sulfide assemblage of MS-158; (c) and (d): The metal-sulfide assemblage MS-166 is a very porous and mineralogically heterogeneous fragment. The sulfide-rich portion (c) contains inclusions of metal (M), fine-grained ureilitic silicates (S), and a coarse-grained olivine grain; the metal-rich area (d) is surrounded by Ni-rich metals and embedded within an intergrowth of Fe-oxide, sulfide (probably troilite; Tr), and minor metal (white); BSE-image. P = pores; M = metals; S = silicates.

Fig. 5: Chondritic lithologies within the Almahata Sitta polymict breccia. (a) MS-11: Distribution of metal/sulfides (white) and silicates (grey) within the H5/6 chondrite fragment; the light grey areas in the upper part are parts of the fusion crust. Pores are black; BSE-image; (b) photomicrograph in transmitted light of the unique chondrite (MS-CH); (c) overview of the Almahata Sitta fragment MS-14, which is an unequilibrated EH3 chondrite (d) photomicrograph in transmitted light of the EL3/4 chondrite (MS-17); (e) the shock-darkened fragment MS-13 is an EH4/5-chondrite; K = kamazite, Old = oldhamite, Nin =

niningerite, FeS = troilite; BSE-image; (f) typical area of the EL6 chondrite MS-52; transmitted light, crossed polarizers.

Fig. 6: Plot of $\delta^{17}O$ vs. $\delta^{18}O$ of Almahata Sitta fragments (solid squares: fine-graine ureilites, solid circles: coarse-grained ureilites, diamonds: enstatite chondrites, triangle: MS-151). The fields of O, E, and R chondrites and ureilites are shown for reference. The average of 3 fragments of MS-CH is displayed for reference (data from Horstmann et al., 2010, this issue).

Fig.1

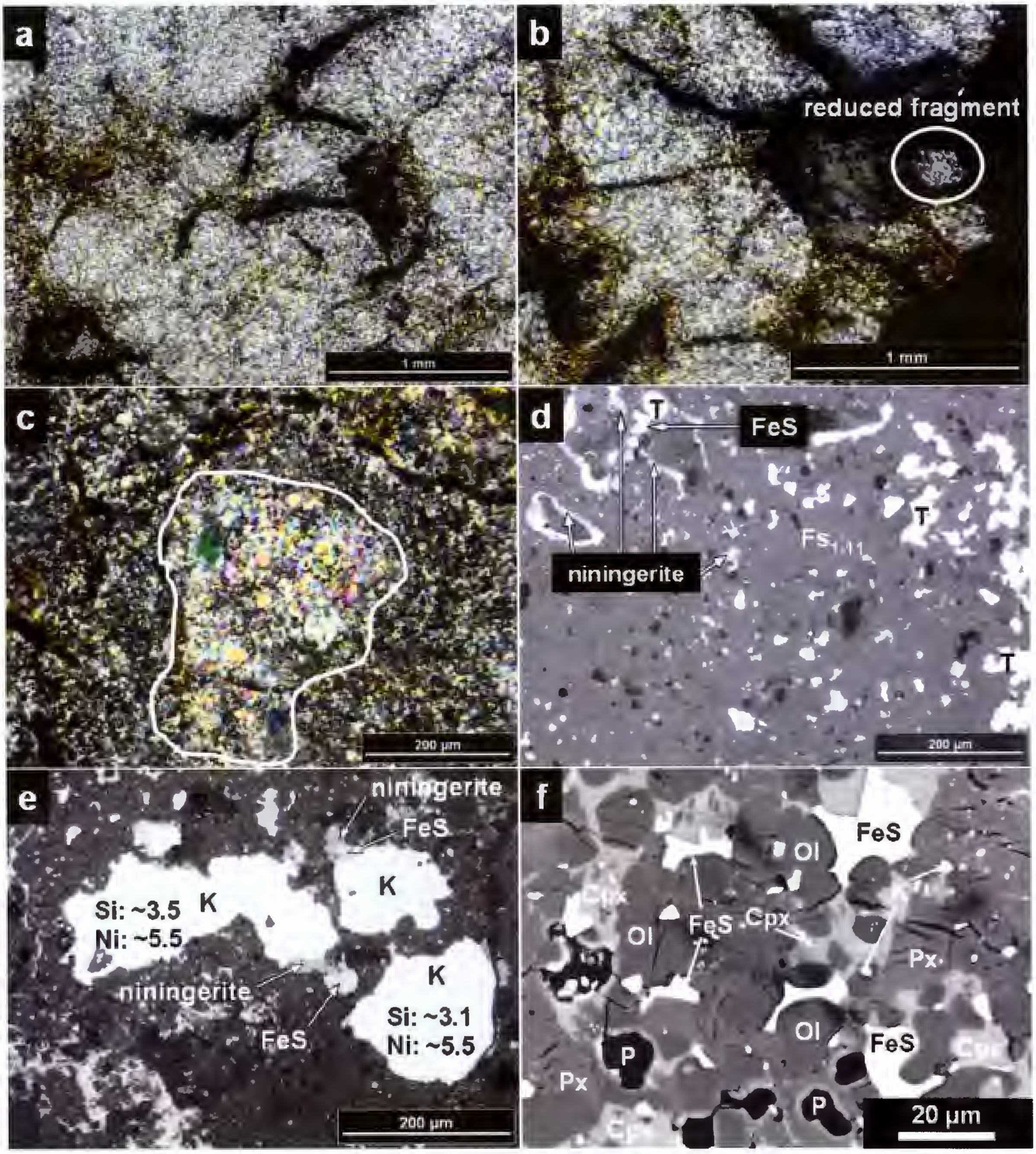

a
1 mm
b
reduced fragment
1 mm
c
200 µm
d
T
FeS
T
niningerite
T
200 µm
e
niningerite
FeS
K
K
Si: ~3.5
Ni: ~5.5
niningerite
FeS
K
Si: ~3.1
Ni: ~5.5
200 µm
f
FeS
Ol
Cpx
Ol
FeS
Cpx
Px
Ol
FeS
P
Px
P
20 µm

Fig.2

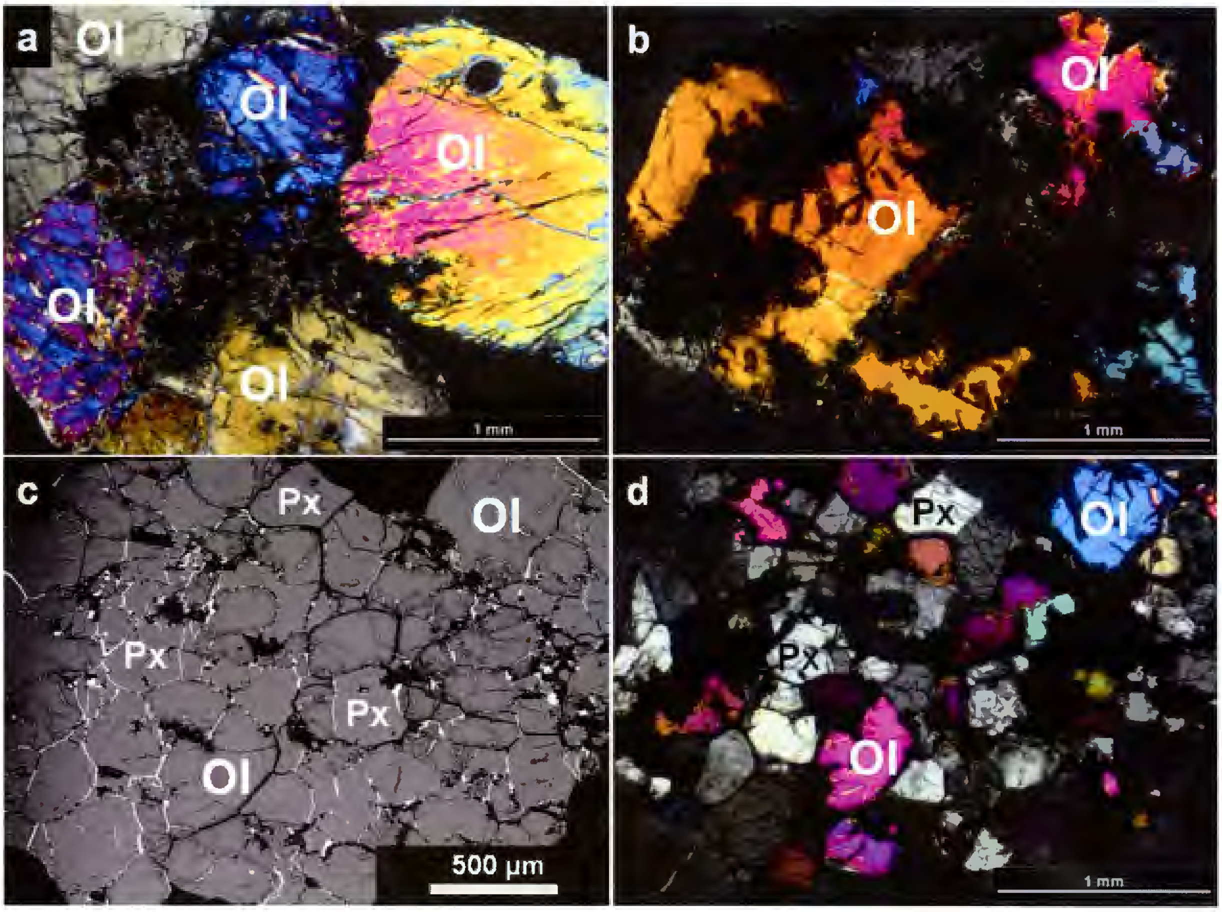
a
Ol
Ol
Ol
Ol
Ol
1 mm
b
Ol
Ol
1 mm
c
Px
Ol
Px
Px
Ol
500 µm
d
Px
Ol
Px
Ol
1 mm

Fig.3

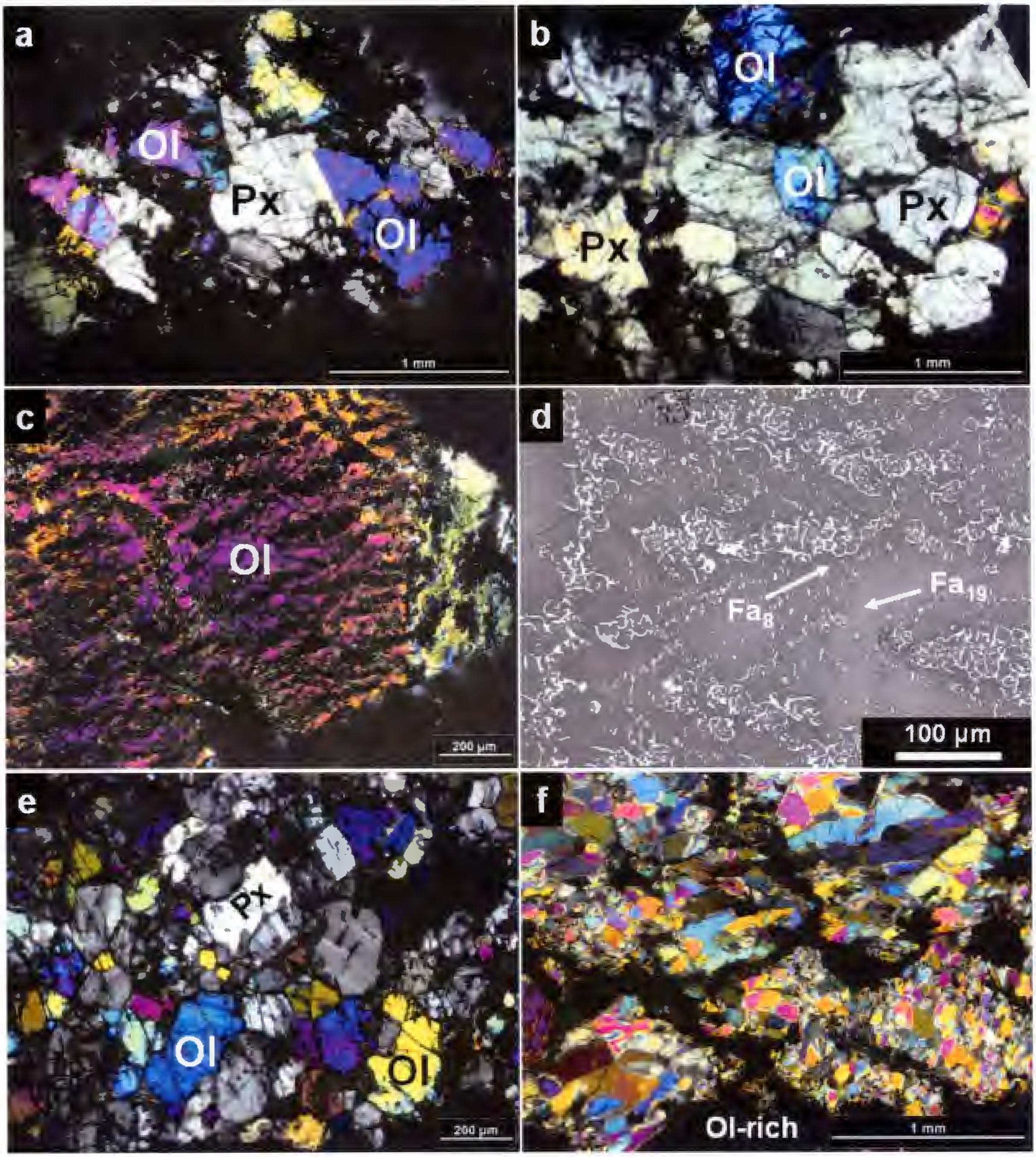

a
Ol
Px
Ol
1 mm
b
Ol
Ol
Px
Px
1 mm
c
Ol
200 μm
d
Fa_8
Fa_{19}
100 μm
e
Px
Ol
Ol
200 μm
f
Ol-rich
1 mm

Fig.4

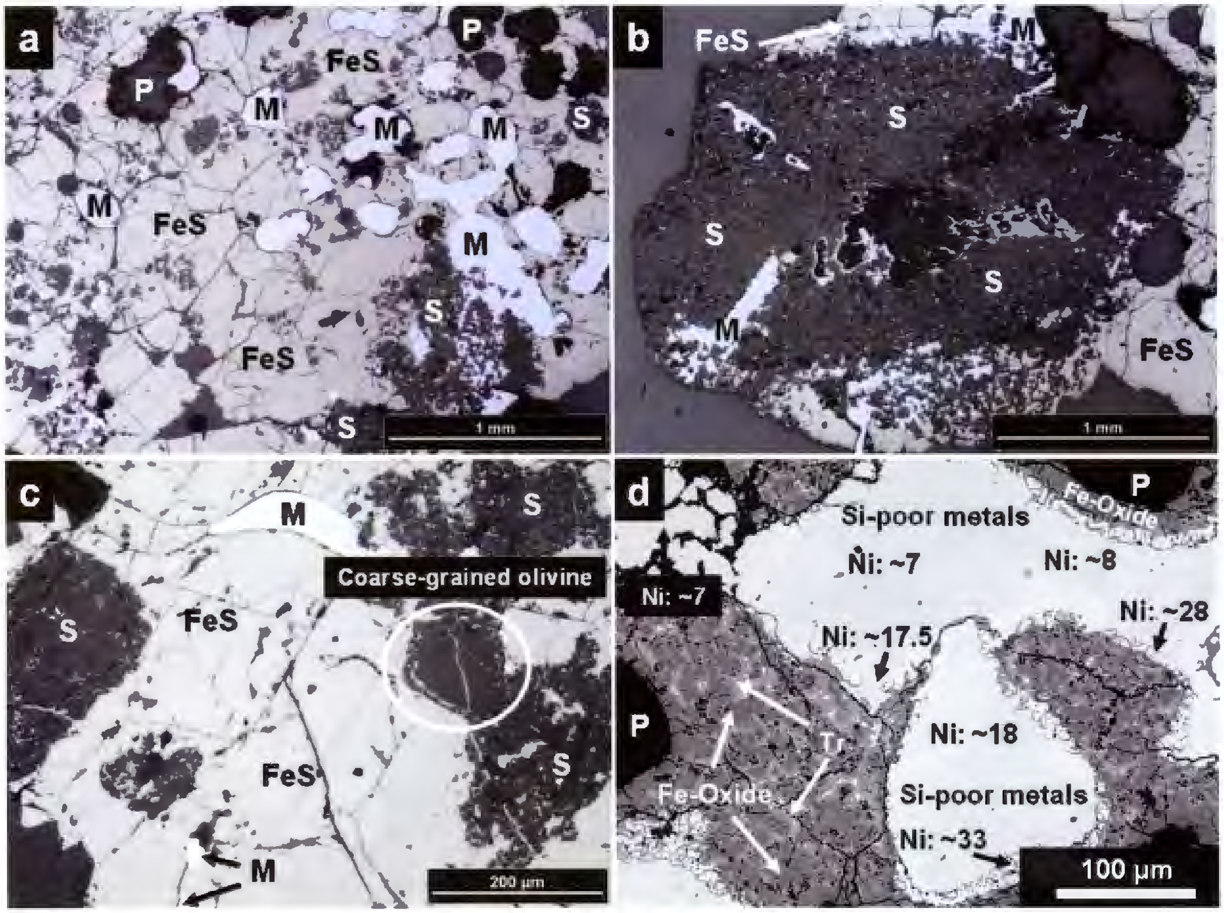
a
P
FeS
P
M
M
M
S
M
FeS
M
S
FeS
S
1 mm
b
FeS
M
S
S
S
M
FeS
1 mm
c
M
S
Coarse-grained olivine
S
FeS
FeS
S
M
200 µm
d
P
Si-poor metals
Fe-Oxide
Ni: ~7
Ni: ~8
Ni: ~7
Ni: ~28
Ni: ~17.5
P
Ni: ~18
Tr
Fe-Oxide
Si-poor metals
Ni: ~33
100 µm

Fig.5

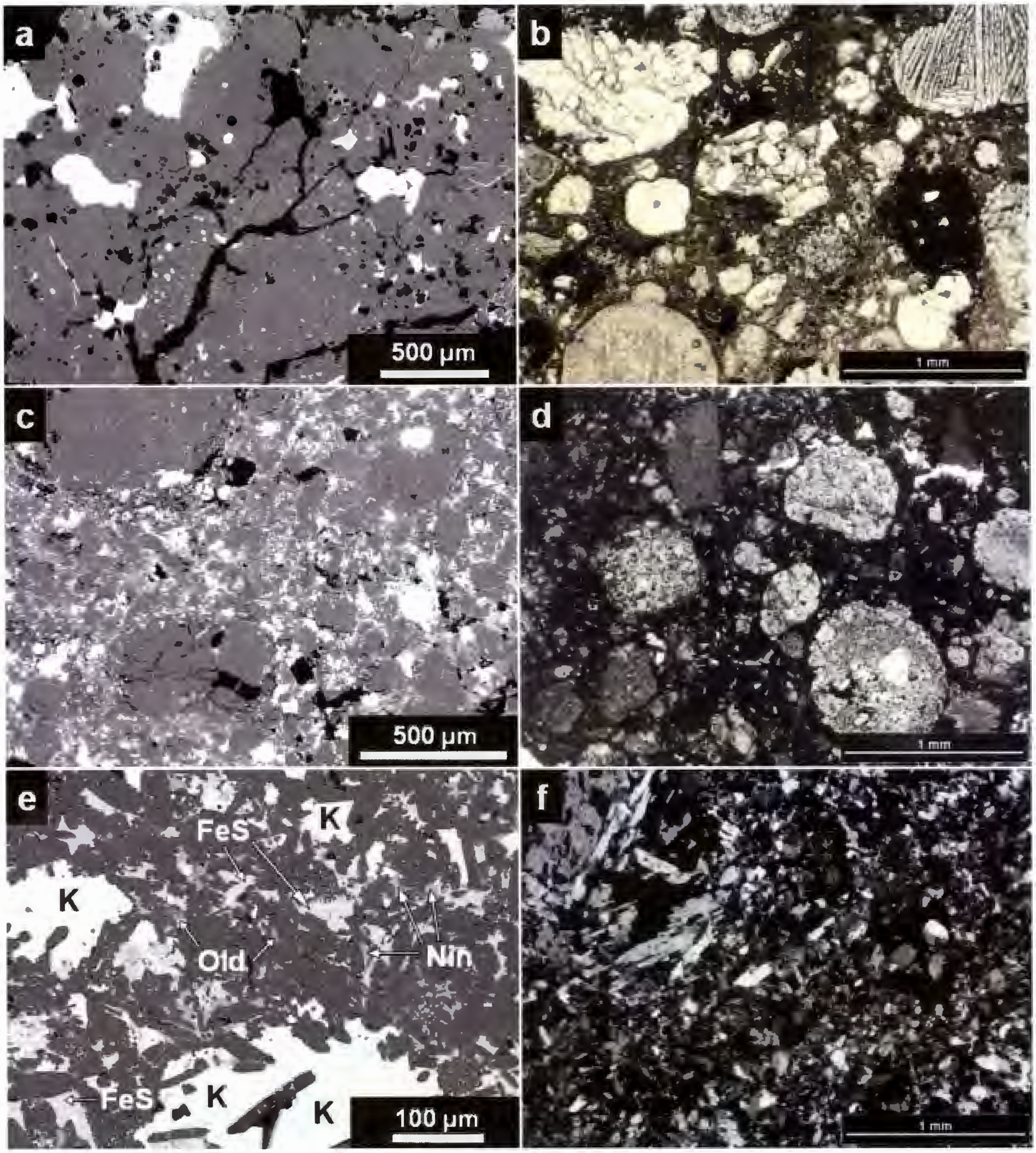

Fig. 6

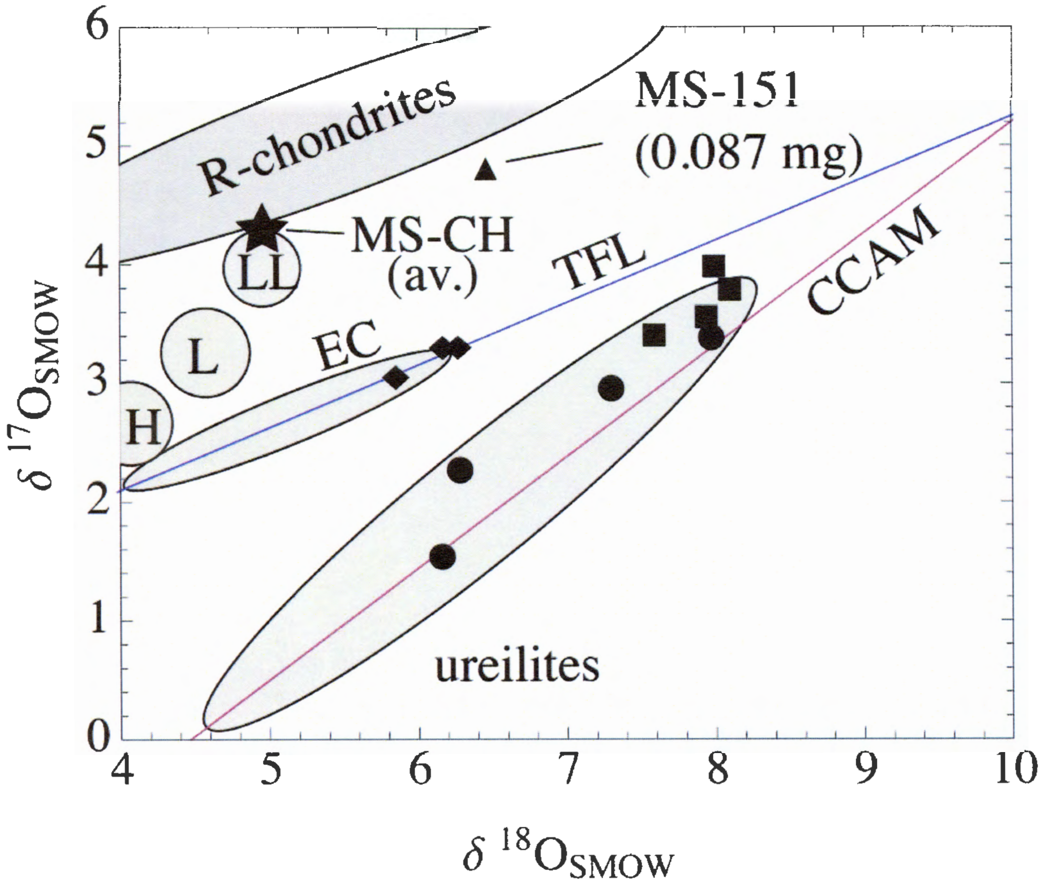

6
5
4
3
2
1
0
4
5
6
7
8
9
10
R-chondrites
MS-151
(0.087 mg)
MS-CH
(av.)
LL
L
H
EC
TFL
CCAM
ureilites
δ 17OSMOW
δ 18OSMOW